PROCEEDINGS B

rspb.royalsocietypublishing.org

Research

Cite this article: Le Floch A, Ropars G. 2017 Left-right asymmetry of the Maxwell spot centroids in adults without and with dyslexia. *Proc. R. Soc. B* **284**: 20171380. http://dx.doi.org/10.1098/rspb.2017.1380

Received: 23 June 2017
Accepted: 22 September 2017

Subject Category:
Behaviour

Subject Areas:
behaviour, neuroscience

Keywords:
optics, asymmetry, human vision, neurological disorders

Author for correspondence:
Guy Ropars
e-mail: guy.ropars@univ-rennes1.fr

Electronic supplementary material is available online at https://dx.doi.org/10.6084/m9.figshare.c.3899371.

THE ROYAL SOCIETY PUBLISHING

Left-right asymmetry of the Maxwell spot centroids in adults without and with dyslexia

Albert Le Floch[1,2,3] and Guy Ropars[1,3]

[1]Laboratoire de Physique des Lasers, UFR SPM, Université de Rennes 1, 35042 Rennes, France
[2]Laboratoire d'Electronique Quantique et Chiralités, 20 Square Marcel Bouget, 35700 Rennes, France
[3]Université Bretagne Loire, 35044 Rennes, France

AL, 0000-0002-4516-9817

In human vision, the brain has to select one view of the world from our two eyes. However, the existence of a clear anatomical asymmetry providing an initial imbalance for normal neural development is still not understood. Using a so-called foveascope, we found that for a cohort of 30 normal adults, the two blue cone-free areas at the centre of the foveas are asymmetrical. The noise-stimulated afterimage dominant eye introduced here corresponds to the circular blue cone-free area, while the non-dominant eye corresponds to the diffuse and irregular elliptical outline. By contrast, we found that this asymmetry is absent or frustrated in a similar cohort of 30 adults with normal ocular status, but with dyslexia, i.e. with visual and phonological deficits. In this case, our results show that the two Maxwell centroid outlines are both circular but lead to an undetermined afterimage dominance with a coexistence of primary and mirror images. The interplay between the lack of asymmetry and the development in the neural maturation of the brain pathways suggests new implications in both fundamental and biomedical sciences.

1. Introduction

Asymmetry is ubiquitous in living beings, including humans, at the molecular and anatomical levels. Although apparently anatomically symmetrical, our two eyes, which are strongly connected to the brain, exhibit rivalry and dominance [1,2]. Besides the crucial role played by genetics and complex molecular mechanisms [3–5], monocular deprivation has shown the importance of competition in the functional development of the complex nervous pathways and synapses, especially during the critical period [1,3–5]. Among the different sense inputs to the human brain, each optic nerve consists of 1.2 million fibres [6], while each auditory nerve a mere 30 000. Deprivation has shown competition between the two eyes from birth [1]. During the so-called critical period, which ends around 8 years of age, each eye sculpts its neural circuit to the brain [3–5]. In normal binocular vision there is an inherent effect of parallax and the brain has to select the eye which is primarily relied on for precise positional information, therefore requiring some hidden asymmetry between the two eyes. The presence or the absence of an asymmetry should play a crucial role in the nervous connectivity for both the visual and the phonological processes in the different modal and cross-modal regions of the brain [7], including from birth [8,9]. Indeed, visual and phonological deficits being involved in dyslexia which affects at least 10% of any given population [10], one may wonder about the role of such asymmetry in this disorder. To unveil this asymmetry, we use here a combination of an afterimage eye dominance determination, and a foveascope technique for a quantitative comparison of the Maxwell spot centroid outlines of the two eyes.

As our two eyes are apparently symmetrical apart from some optical properties, let us concentrate our attention on the foveas from which approximately half of the nerve fibres in the optic nerve carry information to the brain [11]. The

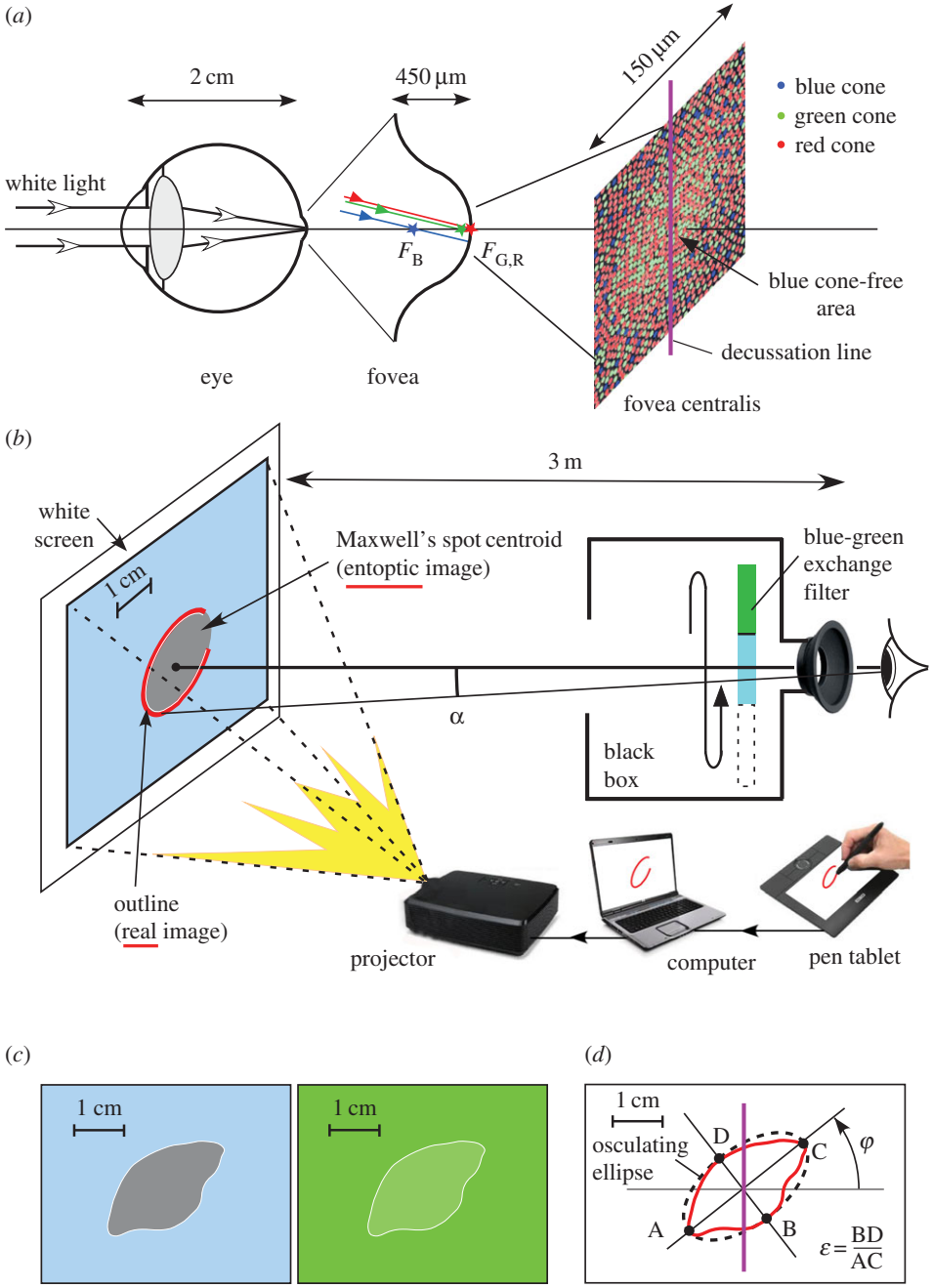

Figure 1. Recording of the two blue cone-free area outlines. (*a*) The blue cone-free area. Owing to the chromatic dispersion, the focusing points for the three types of cones on the fovea are at 17.50, 17.45 and 17.15 mm for the red, green and blue cones respectively, for a normal eye. The vertical decussation line of the retina represented in pink passes at the centre of the fovea [11]. Here the horizontal axis is chosen independently of the actual preferred locus of fixation on the fovea [17]. (*b*) Experimental scheme of the foveascope. For each of the two eyes, the observer compares the outline of the entoptic image corresponding to the blue cone-free area of about 100 µm diameter, with the real image he draws on a pen tablet, which is also projected via a computer on the screen. (*c*) Typical observation for one eye through the blue and green filters. (*d*) Departure from a circular outline measured using the osculating ellipse technique.

arrangement of the photoreceptors on the retina [12] has not the regularity of the pixel spacing of a computer screen. However, they are well aligned with each other on the fovea [13,14]. Moreover, the blue cones play an intriguing role especially in the fovea with their unique distribution and specificity [15]. They are found only outside the fovea centralis [11,16] whereas the green and red cones are concentrated inside (figure 1*a*), and an anatomically distinct pathway conveys their signals to the brain [18]. The blue cones have a peak spectral sensitivity well separated (by about 100 nm) from those of the green and red cones. Owing to chromatic dispersion (figure 1*a*), to preserve the eye acuity in this highly dense receptor area, the human eye has evolved towards a blue cone-free zone of about 100–150 µm in diameter in the cone mosaic of figure 1*a*, which corresponds to the Maxwell spot centroid. Note that, while for the whole Maxwell spot [19] with an overall 1 mm diameter, the macular pigment plays a role, for the small spot centroid the pigment is unable to account for the foveal blue scotoma [20,21,22] which appears as a tiny dark spot (figure 1*b*). The direct observation of the blue cones using anti-blue opsin [16] has unambiguously confirmed the existence of the blue cone-free area at the centre of each fovea, but the analysis has to be made post-mortem. Unfortunately, owing to splitting and swelling in the tissues, a comparison of the outline of the right and left blue cone-free areas for a given subject is then out of reach. We have chosen to build the so-called foveascope to perform a quantitative comparison of the two Maxwell spot centroids of any observer,

including their possible anomalies. We restrict our observation to the centroids where the density of cones and the acuity are the highest [11].

To investigate the presence or the absence of an asymmetry of the blue cone-free areas and a possible link between this asymmetry and the afterimage dominance, we first test a cohort of 30 healthy students. Second, we perform the same tests with a cohort of 30 students with dyslexia, this deficit being characterized by a weaker brain lateralization [23,24]. The preferential use of one eye for visual functions has been debated for a long time. To avoid different sighting artefact, we revisit the ocular dominance by introducing a new method based on the noise-stimulated negative afterimages seen by the brain with the eyes closed.

2. Material and methods

(a) Observers

We tested a first cohort of 30 healthy students from our university with normal binocular vision and no neurological disease (19 males and 11 females). We performed the same tests with a second cohort of 30 students with similar visual status and optical capabilities as the first cohort, but suffering from dyslexia, i.e. with reading difficulties. All dyslexic students had reading performance significantly poorer than expected, and were assessed by their own optometrist to exclude ocular pathology. Subjects were aware of the purpose of the study, but were not told what particular manipulations were made for each trial. Informed consent was obtained from each participant after the explanation of the nature of the study (see the video in the electronic supplementary material). During the academic year, the dyslexic volunteer students (12 males and 18 females), examined by the medical staff of the university, were assisted by the health centre of the university which provided extra-time for the examinations. The degree of impairment between these students varies, but all encountered difficulties in reading, spelling, writing and recognizing left from right. All these students benefit from 30% of extra time for their academic examinations. The entire investigation process was conducted according to the principles expressed in the Declaration of Helsinki.

(b) Foveascope

When an observer looks at a bright white screen through a blue filter, the blue cone-free area at the centre of the fovea is seen as a dark zone on a blue background (figure 1*b*,*c*). For the screen illumination, we use an ACER P1173 projector with a brightness of 3000 lumens. The typical usual fading time of the associated entoptic image is about a few seconds owing to the bleaching of the photoreceptors and the neural adaptation. We have optimized the contrast of the Maxwell centroid entoptic image by using a blue-green exchange filter. The fading time can then be opposed by a periodic shift of this blue-green exchange filter. Through the green filter, the blue cone-free area is seen as a lighter green zone on a dark green background (figure 1*c*). The transmittance of the filters, with 40 nm bandwidths, centred at 460 nm and 535 nm in the blue and the green respectively, is chosen at 16% for the blue filter and 4% for the green filter, leading to a contrasted dark entoptic image (figure 1*b*). Each observer adjusts the modulation frequency between 0.1 to 1 Hz to his best convenience (typically about 0.2 Hz). For each eye, the observer draws the outline of the blue cone-free area by directly superposing the entoptic and the real image projected on the screen (red line in figure 1*b*). Moreover, by comparing the entoptic images to auxiliary calibrated circles also projected on the screen, the angular diameter of the blue cone-free area can be measured. To quantify a possible asymmetry of the two cone-free area outlines, we introduce an osculating ellipse for each eye centroid, and define the ellipticity ε_R and ε_L for the right and the left eye respectively, as defined in figure 1*d*.

(c) Noise-stimulated negative afterimage dominance

Different sighting and sensory methods have been proposed, namely in the last century, to determine the eye preference for an observer. In a first step, we perform the Miles test and the hole-in-the card test reviewed in references [25,26]. However, although there was good test–retest reliability for the two ocular tests, artefacts exist such as the distance of observations or the gaze angle. To avoid any visual artefact, we introduce here a noise-stimulated afterimage method, where the two eyes remain closed after a fixation by the two eyes on a same bright stimulus, i.e. an external object with excellent light reflecting abilities. The observer can look, for instance, at a contrasted window located at about 20 m from the observer (figure 2*a*), or at a black letter like 'b' on a bright screen (figure 6). With his two eyes, the observer gazes at the fixation point schematized by the cross, for a short duration of about 5–15 s according to the light luminance, so as to avoid a too strong saturation of the retina receptors. Then he closes his eyes. The receptors of his two retinas are then equally imprinted. In usual afterimage experiments, when the two eyes are closed after the fixation, the negative afterimage fades in about 6 to 8 s. Moreover, the contribution of each eye to the activation of the afterimage cannot be isolated. However as the neuron responses are nonlinear and exhibit the bistability of resting and spiking states, an external noise is known to enhance the signals of such nonlinear systems [27–29]. For the retinal neurons, the external noise can be provided by the weak diffused light passing through the closed eyelids. So, blocking in a first step the 2 to 3% of the diffused light passing through the eyelids with the hands [30], and then modulating this noise by alternatively shifting the hands in front of each eye, with a periodicity of about 2 s, two noise activations of the afterimage are seen successively for each eye (see the video in the electronic supplementary material). Hence, we have a differential method for comparing the activation in the brain of the same information encoded in the retinas which is part of the central nervous system. The fading time of these activated afterimages is extended to tens of seconds when the successive activations through the eyelids by shifting the hands are continued, and a direct comparison of the luminance and quality of the two activated afterimages is clearly obtained for a given stimulus (figure 2*a*,*b*). Note that in a variant of the method, monocular vision can be used successively for each eye, leading to the same results, thus avoiding any possible binocular fusion problem in the afterimage dominance determination (see the video in the electronic supplementary material). Moreover, as we shall see below, these afterimages appear to be a powerful tool for investigating the consequences of the lack of asymmetry of the foveas in dyslexia, namely in confirming that both an image and its mirror-image can really coexist for dyslexics. For the two cohorts, we will compare the results of the afterimage method with those obtained by the usual sighting methods to determine the ocular dominance.

3. Results

(a) Normal observers

(i) Afterimage dominance

The afterimage tests were performed using the stimulus of figure 2*a*. Typical reconstructions of the observed activated afterimages for each eye are shown in figure 2*a*,*b* for two normal observers. For the first observer no. 5 (figure 2*a*), the afterimage is brighter for the right eye than that for the left eye, while the afterimage brightnesses are interchanged for the second observer no. 17 (figure 2*b*). The results for the

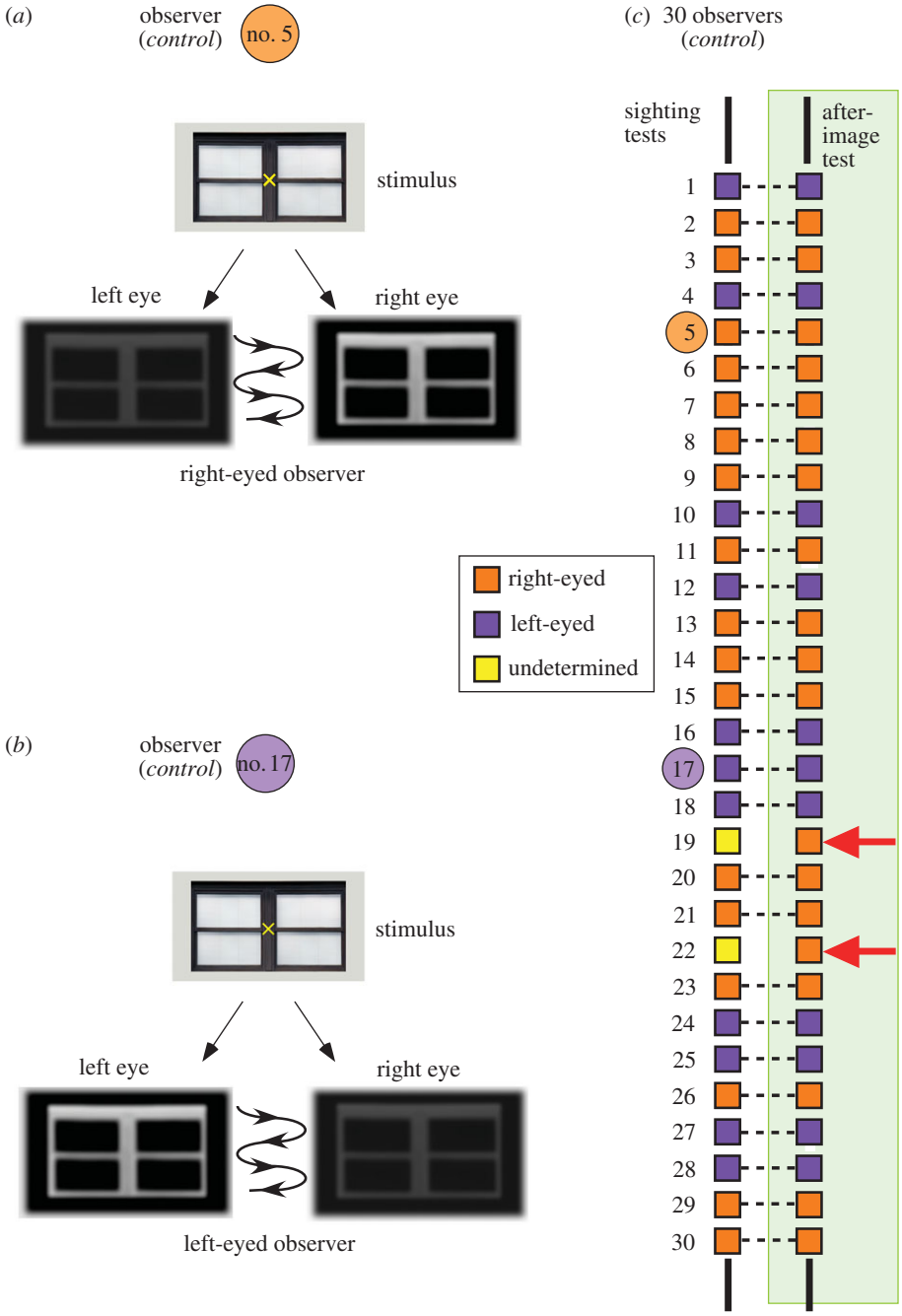

Figure 2. Noise-induced afterimage dominance for the cohort of normal observers. (*a*) The two activated afterimages alternatively seen by the observer no. 5. The strongest activated right-eye afterimage defines the afterimage dominance. The right eye dominance is confirmed by the sighting tests (figure 2*c*). (*b*) The two activated afterimages for the observer no. 17 show a left-eye afterimage dominance, also confirmed by the sighting tests (figure 2*c*). (*c*) Comparative preferred eye observations with the sighting tests and with the afterimage test for the whole cohort of normal observers. For 28 observers, the two methods give identical results (noted by the dotted lines). For the observers nos 19 and 22, the gaze effect perturbs the sighting tests but the afterimage test leads to a clear right-eye dominance.

whole cohort are shown in the right column of figure 2*c*. In parallel, the observers have tested their ocular dominance using the Miles and the hole-in-the card tests. The results are shown in the left column of figure 2*c*. For the cohort of 30 normal observers, the sighting tests determine the eye dominance for 28 observers (figure 2). Only two observers (nos 19 and 22) have no eye dominance, owing to gaze incidence problems. The afterimage method confirms the eye preference of the 28 observers, and determines also the eye dominance of the observers nos 19 and 22. Hence, in absence of any visual artefact, the noise-stimulated afterimage method unambiguously determines the eye dominance for the whole cohort. Sixty-three per cent of the students were right-eyed dominant, while 36% were left-eyed dominant (represented in orange and purple respectively in figure 2*c*). These results are robust and generally confirm the usual sighting tests. Moreover, note that the afterimage test clearly suggests that the neural connections of one retina to the brain are stronger than those from the other retina. The level of significance of the dominance is reinforced by earlier measurement of the shorter reaction time of the dominant eye [31] and by functional magnetic resonance imaging where the dominant eye activates a larger area and a higher signal of the primary visual cortex than the non-dominant eye [32]. However, the basic question of the origin of the ocular dominance remains to be answered. To look for a possible link with a potential asymmetry of the blue cone-free areas, we investigated the Maxwell centroid outlines of the whole cohort of 30 healthy students.

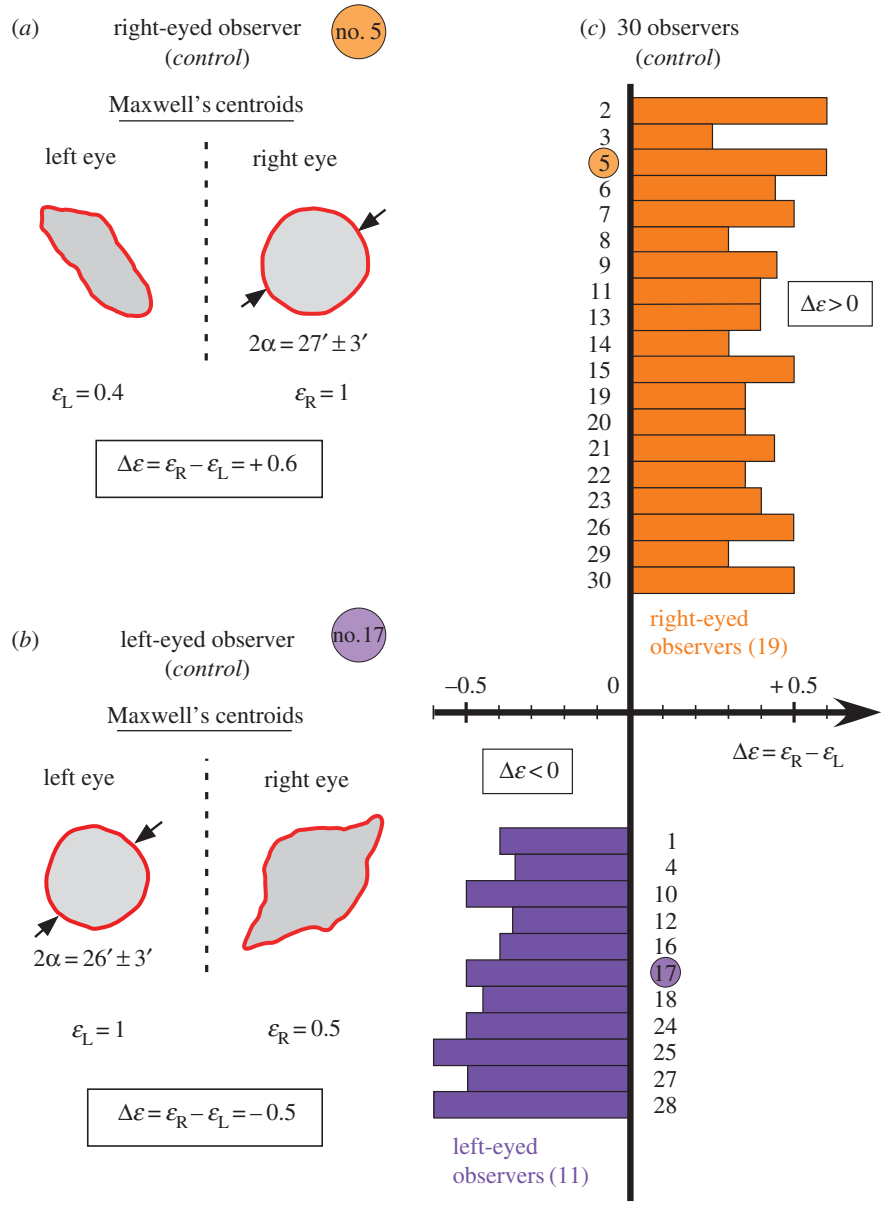

Figure 3. Maxwell's centroid asymmetry measured by the control cohort. The right and the left eyed observers of figure 2 have been gathered. (*a*) Asymmetry of Maxwell's outlines for the right-eyed observer no. 5. (*b*) Reversed asymmetry for the left-eyed observer no. 17. (*c*) The positive asymmetry measurements for the 19 right-eyed observers (noted in orange) and the negative asymmetry measurements for the 11 left-eyed observers (noted in purple).

(ii) Maxwell's spot centroids asymmetry

The recording of the outlines of the Maxwell centroids using the foveascope is performed by each normal observer of the cohort, independently of the afterimage dominance test. The typical results for the outline measurements of the Maxwell centroids are shown in figure 3*a* for the right-eyed observer no. 5 and in figure 3*b* for the left-eyed observer no. 17. The asymmetry between the two outlines for each observer is clear and quantified by the coefficient of asymmetry $\Delta\varepsilon = \varepsilon_R - \varepsilon_L$. The main results for the whole cohort of the normal observers shown in figure 3*c* are: first, the existence of an asymmetry for all observers, and second, a reversed sign of the coefficient of asymmetry between the right and left-eyed groups. For the right-eyed observers, the coefficient of asymmetry is systematically positive, with a mean value $\langle\Delta\varepsilon\rangle = +0.42$, while for the left-eyed observers, the asymmetry coefficient is negative with a mean value $\langle\Delta\varepsilon\rangle = -0.47$. The mean angular diameter of the centroids for the observers is $\langle 2\alpha\rangle = 27' \pm 3'$ and there is no preferred azimuth φ (figure 1*d*) for the elliptical outline. Moreover, the dominant eye with its stronger connectivity to the brain is likely to be determined by the circular outline centred on the decussation line (figure 1*a*), and the non-dominant eye by the elliptical and somewhat irregular outline. The asymmetry coefficient corresponding to two different topographies of the blue cones, varies from $|\Delta\varepsilon| = 0.3$ (weak asymmetry) to $|\Delta\varepsilon| = 0.6$ (strong asymmetry), but the correlation between the blue cone-free area asymmetry and the afterimage dominance is perfect for the 30 students.

(b) Dyslexic observers

(i) Afterimage dominance

Figure 4*a* shows the observations with the afterimage test, for the observer no. 15. The two eyes show two identical activated afterimages for this observer. Such undefined afterimage dominance is seen for 27 observers of the cohort (figure 4*b*). As for the cohort of normal observers, we have investigated the ocular dominance of the cohort of students with dyslexia, using the Miles and hole-in-the-card tests. The results reported in the left column of figure 4*b* show that the sighting tests gave

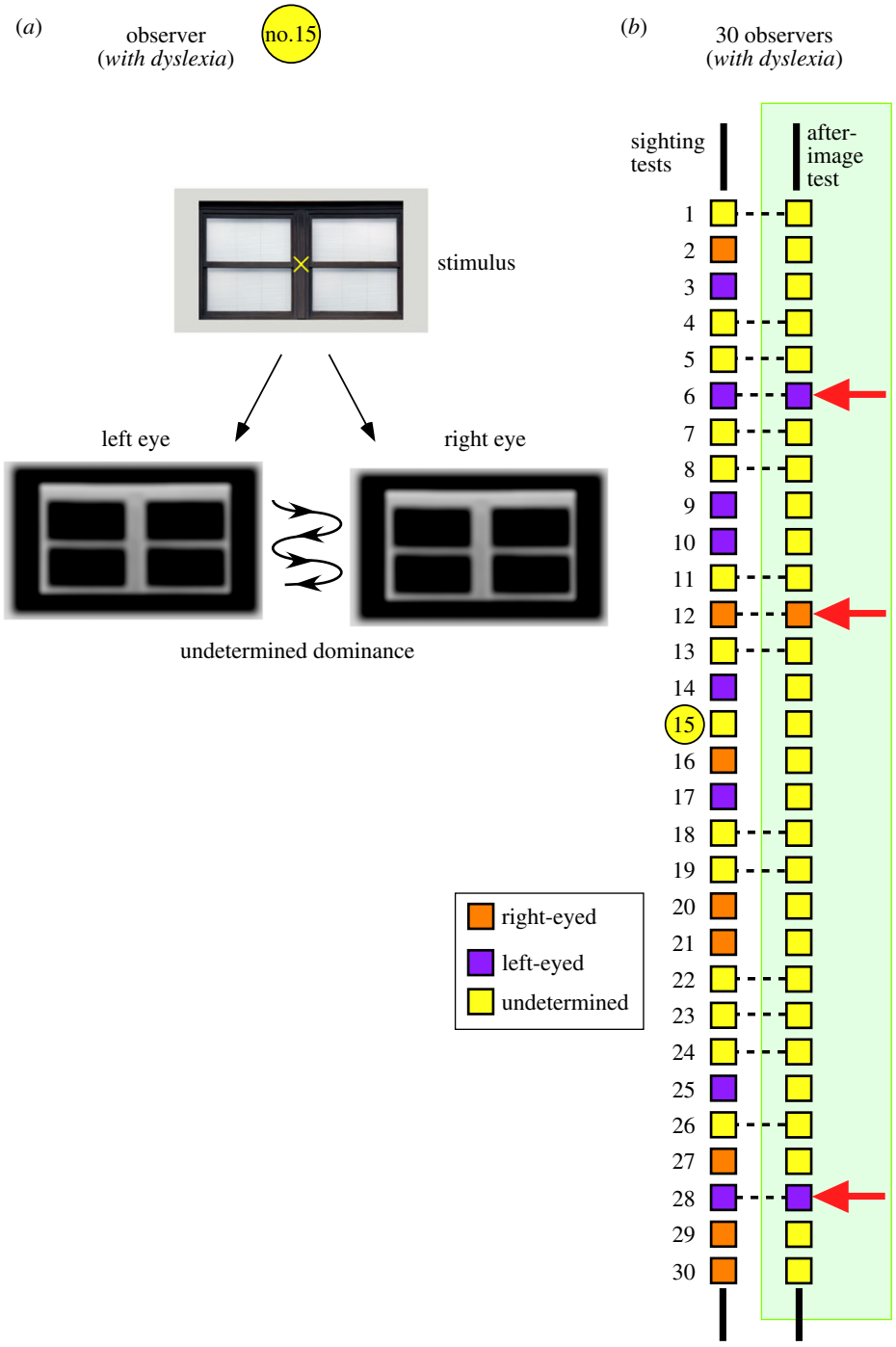

Figure 4. Noise-induced afterimage dominance for the cohort of observers with dyslexia. (*a*) The two activated afterimages for the observer no. 15 with dyslexia. The two afterimages have the same luminance. For this observer, the afterimage dominance is undetermined, in agreement with the sighting tests. (*b*) Comparative preferred eye observations with the sighting tests and with the afterimage test for the whole cohort of observers with dyslexia. For 16 observers, the two methods give identical results (noted by the dotted lines). For the other 14 observers, the afterimage test gives an undetermined dominance, although the sighting tests, with their possible artefacts, give an apparent dominance. In short, for this cohort, all observers show an undetermined afterimage dominance, apart from observer nos 6, 12 and 28 who have a robust dominance with both the sighting and afterimage tests (see figure 5*b* and the text).

more difficulties than for the cohort of normal observers. Indeed, for 14 observers, the sighting tests give an apparent dominance probably linked to the gaze of incidence. The results can vary throughout the day or from day to day. For these 14 observers the difficulties vanish with the afterimage test (see the right column in figure 3*b*). For the other 16 observers, noted by the dotted lines, the two methods give identical results. For 13 of these observers, no ocular dominance exists. However, three students in the cohort (nos 6, 12, 28) have a dominant eye both with the sighting tests and the afterimage test. These particular cases are discussed below. Finally 27 observers in the whole cohort of students with dyslexia exhibit an undetermined afterimage dominance.

(ii) Maxwell's spot centroid asymmetry

Let us investigate the centroid outlines for these 27 dyslexic students without any ocular dominance and for the three special cases. For the observer no. 15 for instance, the two outlines represented in figure 5*a* show a lack of asymmetry $\varepsilon_R \simeq \varepsilon_L \simeq 1$. This lack of asymmetry is systematically observed for the 27 observers of the cohort with an undefined afterimage

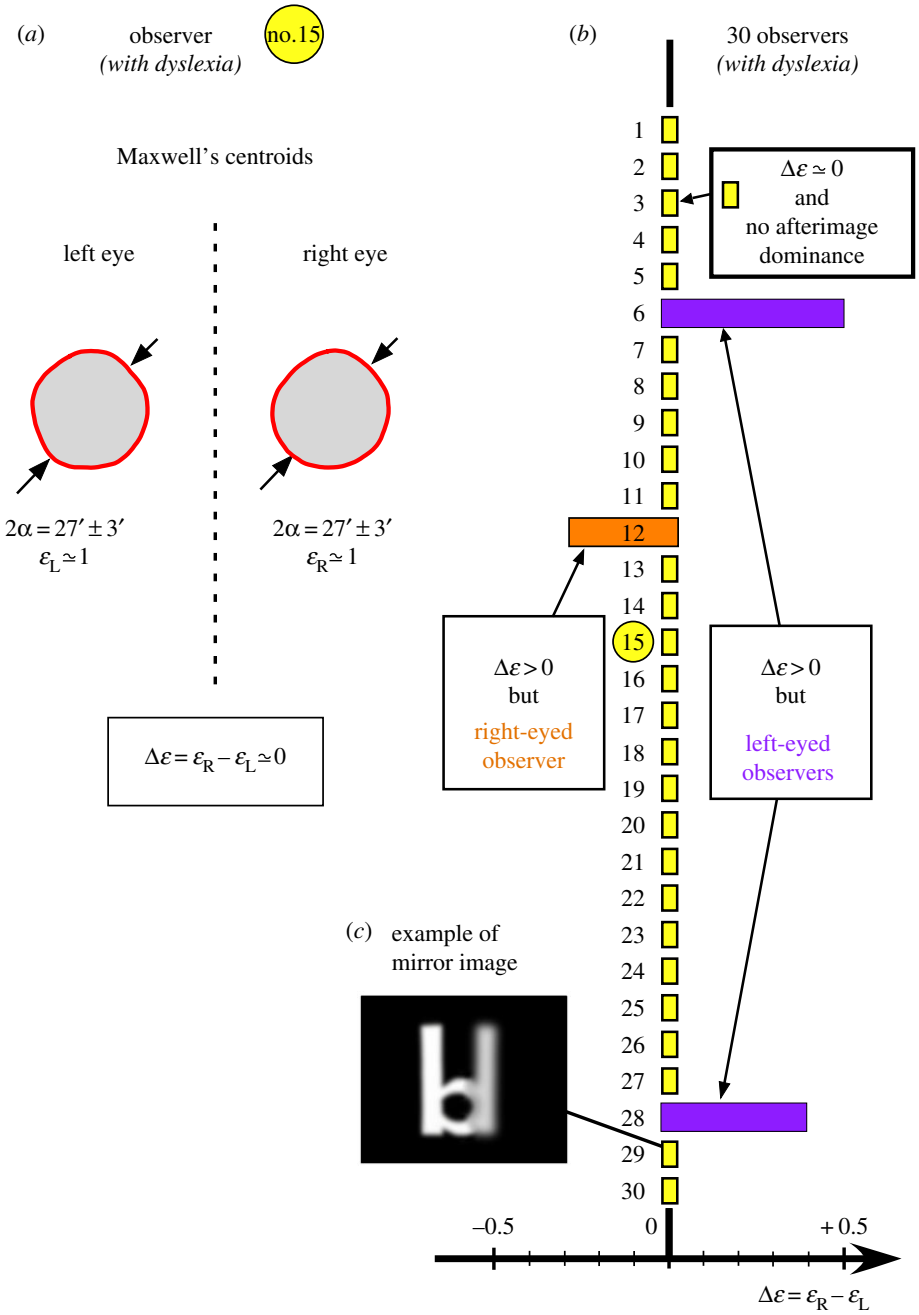

Figure 5. Maxwell's centroid asymmetry measured by the 30 observers with dyslexia. (*a*) The blue cone-free area outlines for the same observer no. 15 with dyslexia. The asymmetry of the outlines disappears. The two outlines are quasi circular with $\varepsilon_R \simeq \varepsilon_L \simeq 1$. (*b*) Results for the cohort of observers with dyslexia: 27 of the 30 observers were unable to detect any asymmetry ($\Delta\varepsilon = \varepsilon_R - \varepsilon_L \simeq 0$). The three observers no. 6, no. 12 and no. 28 have a frustrated dominance (see text). The right and left dominance are also represented in orange and purple respectively as in figure 2. (*c*) Example of coexistence of the afterimage 'b' and of its mirror-image 'd' seen by the observer no. 29 with dyslexia (see also figure 6 and the electronic supplementary material, figures S1 and S2 for other observers with dyslexia).

dominance (figure 5*b*). However, the mean angular diameter $\langle 2\alpha \rangle$ for this cohort is similar to that in the controls. Surprisingly, the three students (nos 6, 12, 28) with an afterimage dominant eye have a clear asymmetry of their outlines (figure 5), comparable to that of the controls. However, by contrast, here their dominant eye corresponds to the elliptical outline and not to the circular one, which was the case for the cohort of normal observers. In fact, these three students (nos 6, 12, 28) have had a 'frustrated' dominance since their birth owing to strabismus, severe amblyopia, and facial malformations respectively, unfortunately affecting their eye with the circular outline. So, apart for the three students with frustrated afterimage dominance, for all the students with dyslexia, the undefined afterimage dominance exists and is correlated with the lack of asymmetry (figure 5*b*).

(iii) Coexistence of primary image and mirror image

The lack of asymmetry of the blue cone topographies described above in the two eyes of dyslexics is likely to result in unexpected consequences. Dyslexics confuse left and right and often make mirror errors in reading [33–38]. In particular mirror-image letters along the vertical line, such as the 'b' and the 'd', are often confused. The neurological basis of such letter reversal remains unknown. Repeating the afterimage test with the letter 'b' as a stimulus, for instance the observer no. 29 with dyslexia sees a superposition of 'b' and 'd' (figures 5*c* and 6*c*). Surprisingly, in contrast to the case of a normal observer (figure 6*b*), for this observer no. 29 the true image 'b' and the mirror image 'd' coexist, explaining his basic confusion and his basic reading difficulties. However,

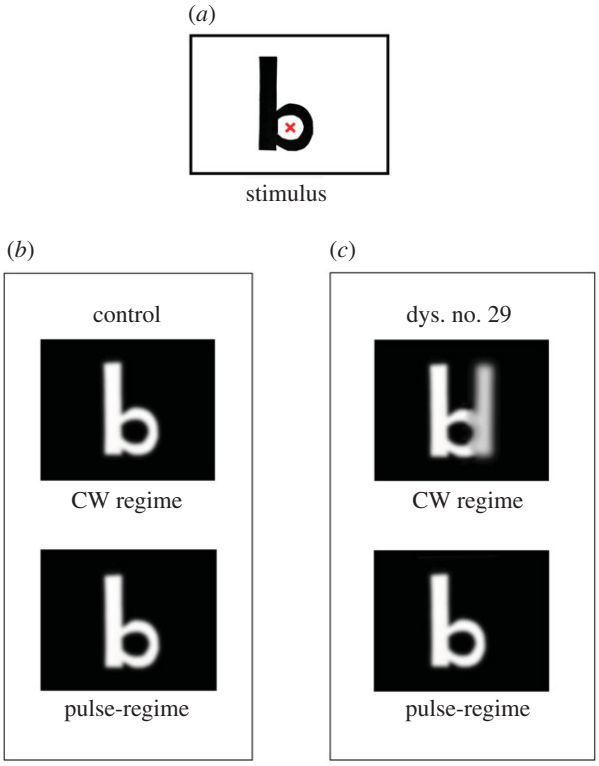

Figure 6. Comparative afterimages of an asymmetric letter for an observer without dyslexia and for an observer with dyslexia (no. 29). (*a*) Scheme of the asymmetric letter 'b' used as stimulus, with its fixation point (red cross). (*b*) Reconstructed afterimages observed by a control using a continuous wave (CW lamp) to light the stimulus (top) and a pulse-width modulation light-emitting diode (bottom). (*c*) Reconstructed afterimages observed by the dyslexic observer no. 29. While the control sees the expected negative afterimage 'b' in the CW regime, surprisingly, in this regime, the dyslexic student sees a superposition of the initial letter 'b' and also its mirror image 'd' (top). Amazingly, using a pulse-width modulation light-emitting diode (modulation frequency equal 70 Hz, duty cycle of 20%, no visible flickering), the extra mirror-image 'd' is suppressed (bottom) and the reading skills are restored. Similar results with spurious extra mirror-images are shown for other students with dyslexia in the electronic supplementary material, figures S1 and S2.

when the brain of the dyslexic reads the superposition of 'b' and 'd', a delay of about 5–10 ms exists for the arrival of the mirror-image 'd' which has an extra-path through the corpus callosum [33]. This small delay suggests the possibility of erasing this secondary mirror-image 'd' using the critical temporal window [39] for depressing the synapses producing the mirror image, according to the Hebbian mechanism. We can exploit this delay to achieve the mirror breaking, i.e. to suppress the mirror image, as in normal observers. Indeed, for the dyslexic observer no. 29, using a pulse-width-modulation light-emitting diode taking advantage of the small delay, the afterimage test directly shows that the spurious apparition of the mirror image 'd' is actually cancelled (figure 6*c*). Interestingly, with no visible flickering (above about 70 Hz), the normal reading skills are restored for this observer, as for other observers with dyslexia. For observers nos 3 and 16, the lateral shifts of the different spurious mirror afterimages are larger (electronic supplementary material, figure S1*b*) or more complex (electronic supplementary material, figure S1*c*), while for the observers nos 22 and 24, other letters like c appear with their mirror images at different locations (electronic supplementary material, figures S2*b* and S2*c*).

(iv) Results for a whole family

The presence or absence of asymmetry in foveas at birth and throughout development seems to play a pivotal role in the neural connectivity of the brain for both cohorts. Family and twin studies [40] have shown that genetics plays an important role, inducing heritability of dyslexia [41]. However the link between genes and phenotypes is particularly precarious in complex disorders such as developmental dyslexia which corresponds to a heterogeneous condition. Different researchers have independently identified several susceptibility genes for dyslexia pointing towards molecular pathways affecting neuronal migration and axon guidance [41]. We have had the opportunity to test the asymmetry and the afterimage dominance in the whole family of observer no. 29. The blue cone-free areas of the five members medically detected with dyslexia are shown in electronic supplementary material, figure S3. For all members, no asymmetry is present, and the afterimage dominance is undetermined, suggesting a genetic cause. The presence or the absence of asymmetry of the two blue cone-free areas seems a promising direction for trying to identify the related genes in dyslexia. Families with affected and unaffected members are perhaps the best candidates for such investigations.

4. Discussion and conclusion

(a) Asymmetry, dominance and visual pathways

Hence, for normal observers, the two topographies of the blue cones associated with the asymmetry of the outlines are different for the two eyes and the distribution of the green and red cones are also necessarily differently perturbed, namely at the centre of the fovea. Consequently, the two retinal images are therefore also slightly different. The more regular distribution of photoreceptors on the fovea of the dominant eye suggests a better retinal image quality for this eye. Moreover, the circular blue cone-free area of the afterimage dominant eye preserves its own symmetry in relation to the vertical decussation line passing through its centre. Hence, the necessary cementing of the nasal and temporal half-fields of the retinas projected on the two hemispheres for each eye [42] via the corpus callosum, is easier for the dominant eye. This cementing is facilitated by the more similar receptive structures associated with the two halves of the circular profiles separated by the decussation line, then leading to a shorter reaction time for the dominant eye as observed earlier [31]. More importantly, as the brain circuits are remodelled by use, owing to synaptic plasticity, namely during their developmental critical period (0–8 years), the asymmetry is also reinforced and gradually transferred to the brain through the retinotopic organization of the visual cortex [43]. A longitudinal study has shown that the robustness of the dominance is also increased during this period [44] where the asymmetry contributes to the complex operations that assemble the cortical circuits in the numerous areas of the brain and to the lateralization, essential for reading [23,24,37]. Note that it is only at the end of the developmental period of about 8 years, that the child eye dominance is concomitantly stabilized with a decrease of the mirror reversal errors [34].

For dyslexic students, their two eyes are equivalent and their brain has to successively rely on the two slightly different versions of a given visual scene, moreover often inducing poor and unstable fixation [45]. The lack of asymmetry in

dyslexics perturbs the complex connectivity and lateralization of the different modal and cross-modal regions of the brain involved in reading and other tasks. The retinal connectivity [46], the organization [47] and the detailed topography [43] of the primary cortex, along with the columnar architecture [48] can be affected, but also numerous superior bundles such as the corpus callosum [49], the magnocellular pathway [50], and the left arcuate fasciculus where converging cross-modal interaction of phonemes and graphemes is observed [7]. A whole-brain functional connectivity analysis of dyslexia [24] confirms that dyslexics show a decreased connectivity along the visual pathway as well as between visual and prefrontal regions. The weak lateralization is confirmed by functional transcranial Doppler ultrasound [23].

(b) Mirror-image confusion in dyslexia

Mirror-image confusion is common in many species such as pigeons, dogs, monkeys [51,52]. The phenomenon is also observed in humans, namely in young children and dyslexics [34–38], although all with normal ocular status [53]. However, although the experimental tests have been performed with several visual presentation conditions of stimulus, the neural mechanisms remain largely unknown. The bilateral symmetry of the nervous system with inter-hemispheric pathways linking homologue points are critical to mirror-image confusion. Reading requires distinguishing mirror letters such as 'b' and 'd'. The asymmetry of the topographies of the cones observed on the two foveas in a subject without dyslexia, necessarily induces small differences between the quality of the two retinal images and between the qualities of the corresponding retinotopic maps of the visual cortex hemispheres. Moreover, one can speculate that the secondary mirror images resulting from the inter-hemispheric projections which are in competition with the primary images, are necessarily slightly degraded owing to the asymmetry and thus cancelled by the brain (figure 6*b*).

By contrast, for an observer with dyslexia, the Maxwell centroids are both quasi circular and the two cone topographies are more regular and similar, so that the primary and the mirror-image can have the same quality and luminance. As shown in figure 6, the mirror-image is not seen by the control, but is seen for example by the observer no. 29 with dyslexia. The primary afterimage and the mirror-afterimage coexist for this dyslexic (figure 6*c*), inducing confusion and affecting his reading skills. The afterimages of electronic supplementary material, figures S1*b*,*c* and S2*b*,*c* seen by other observers with dyslexia (no. 3, no. 16, no. 22 and no. 24), show that the mirror inter-hemispheric projections also exist for these observers, but can be slightly deviated and distorted for different letters. Furthermore, as dyslexics are also confronted with unstable binocular fixation [45], their observed afterimages can be even more complex, as for example the triple 'b' seen by observer no. 16 (electronic supplementary material, figure S1*c*). For all these observers with dyslexia the pulse-width modulation light-emitting diode, exploiting the small delay between the primary and mirror images, erases the perturbing extra-images at frequencies where no visible flickering occurs (i.e. around 70 Hz) and restores the reading skills.

(c) Conclusion

The noise-induced negative afterimage method enables us to determine the ocular dominance for an observer, which is correlated with the asymmetry of the outlines of the Maxwell spot centroids. Beyond genetics, the asymmetry between the two blue cone-free areas appears to be a necessary and fundamental condition for brain connectivity for a normal development. By contrast, the lack of asymmetry might be the biological and anatomical basis of reading and spelling disabilities in people with a normal ocular status but with dyslexia, perturbing the connectivity of different regions in the brain and inducing the observed common visual and phonological difficulties [54–56]. Our results suggest early anatomical diagnosis of dyslexia in young children and possible compensation for their potential lack of asymmetry, especially during the critical period. For adults, opportunities such as exploiting the small delays in the brain connections by using pulse-width modulation light-emitting diodes may provide novel strategies to overcome reading and other neurological difficulties.

Ethics. This study was conducted according to the principles expressed in the Declaration of Helsinki.

Data accessibility. This article has no additional data.

Authors' contributions. A.L.F. designed the study and wrote the manuscript. G.R. and A.L.F. performed the experiments. The two authors contributed to the interpretation of the data, discussed the results and commented on the manuscript.

Competing interests. We have no competing interests.

Funding. We received no funding for this study.

Acknowledgements. We would like to thank the kind participation of the students of the two cohorts and of the families. The authors gratefully acknowledge the support of the 'Pôle Handicap' of the Universities of Rennes 1 and Rennes 2, and the technical assistance of J. R. Thébault. We acknowledge B. Beutler for his suggestions in genetics.

References

1. Wiesel TN, Hubel DH. 1963 Single-cell responses in striate cortex of kittens depraved of vision in one eye. *J. Neurophysiol.* **26**, 1003–1017.
2. Haynes JD, Deichmann R, Rees G. 2005 Eye-specific effects of binocular rivalry in the human lateral geniculate nucleus. *Nature* **438**, 496–499. (doi:10.1038/nature04169)
3. Morishita H, Miwa JM, Heintz N, Hensch T. 2010 Lynx1, a cholinergic brake, limits plasticity in adult visual cortex. *Science* **330**, 1238–1240. (doi:10.1126/science.1195320)
4. Southwell DG, Froemke RC, Alvarez-Buylla A, Stryker MP, Gandhi SP. 2010 Cortical plasticity induced by inhibitory neuron transplantation. *Science* **327**, 1145–1148. (doi:10.1126/science.1183962)
5. Lee H, Brott BK, Kirkby LA, Adelson JD, Cheng S, Feller MB, Datwani A, Shatz CJ. 2014 Synapse elimination and learning rules co-regulated by MHC class I H2-D^{b}. *Nature* **509**, 195–200. (doi:10.1038/nature13154)
6. Jonas JB, Schmidt AM, Müller-Bergh JA, Schlötzer-Schrehardt UM, Naumann GOH. 1992 Human optic nerve fiber count and optic disc size. *Invest. Ophth. Vis. Sci.* **33**, 2012–2018.
7. Gullick MM, Booth JR. 2014 Individual differences in crossmodal brain activity predict arcuate fasciculus connectivity in developing readers. *J. Cogn. Neurosci.* **26**, 1331–1346. (doi:10.1162/jocn_a_00581)
8. Gomez J, Barnett MA, Natu V, Mezer A, Palomero-Gallagher N, Weiner KS, Amunts K, Zilles K, Grill-Spector K. 2017 Microstructural proliferation in human cortex is coupled with the development of

face processing. *Science* **355**, 68–71. (doi:10.1126/science.aag0311)
9. Deen B, Richardson H, Dilks DD, Takahashi A, Keil B, Wald LL, Kanwisher N, Saxe R. 2017 Organization of high-level visual cortex in human infants. *Nat. Commun.* **8**, 13995. (doi:10.1038/ncomms13995)
10. Sprenger-Charolles L, Siegel LS, Jiménez JE, Ziegler JC. 2011 Prevalence and reliability of phonological, surface and mixed profiles in dyslexia: a review of studies conducted in languages varying in orthographic depth. *Sci. Stud. Read.* **15**, 498–521. (doi:10.1080/10888438.2010.524463)
11. Rodieck RW. 1998 *The first steps in seeing*. Sunderland, MA: Sinauer Associates.
12. Roorda A, Williams DR. 1999 The arrangement of the three cone classes in the living human eye. *Nature* **397**, 520–522. (doi:10.1038/17383)
13. Roorda A, Williams DR. 2002 Optical fiber properties of individual human cones. *J. Vis.* **2**, 404–412. (doi:10.1167/2.5.4)
14. Le Floch A, Ropars G, Enoch J, Lakshminarayanan V. 2010 The polarization sense in human vision. *Vision Res.* **50**, 2048–2054. (doi:10.1016/j.visres.2010.07.007)
15. Martin PR, Lee BB. 2014 Distribution and specificity of S-cone (blue cone) signals in subcortical visual pathways. *Vis. Neurosci.* **31**, 177–187. (doi:10.1017/S0952523813000631)
16. Curcio CA, Allen KA, Sloan KR, Lerea CL, Hurley JB, Klock IB, Milam AH. 1991 Distribution and morphology of human cone photoreceptors stained with anti-blue opsin. *J. Comp. Neurol.* **312**, 610–624. (doi:10.1002/cne.903120411)
17. Putnam NM, Hofer HJ, Doble N, Chen L, Carroll J, Williams DR. 2005 The locus of fixation and the foveal cone mosaic. *J. Vis.* **5**, 632–639. (doi:10.1167/5.7.3)
18. Dacey DM, Lee BB. 1994 The 'blue-on' opponent pathway in primate retina originates from a distinct bistratified ganglion cell type. *Nature* **367**, 731–735. (doi:10.1038/367731a0)
19. Maxwell JC. 1856 On the unequal sensitivity of the foramen centrale to light of different colors. *Athenaeum* **1505**, 1093.
20. Isobe K, Motokawa K. 1955 Functional structure of the retinal fovea and Maxwell's spot. *Nature* **175**, 306–307. (doi:10.1038/175306a0)
21. Williams DR, MacLeod DI, Hayhoe MM. 1981 Foveal tritanopia. *Vision Res.* **21**, 1341–1356. (doi:10.1016/0042-6989(81)90241-8)
22. Magnussen S, Spillmann L, Stürzel F, Werner JS. 2004 Unveiling the foveal scotoma through the afterimage. *Vision Res.* **44**, 377–383. (doi:10.1016/S0042-6989(01)00178-X)
23. Bishop DVM. 2013 Cerebral asymmetry and language development: cause, correlate, or consequence? *Science* **340**, 1230531. (doi:10.1126/science.1230531)
24. Finn ES, Shen X, Holahan JM, Scheinost D, Lacadie C, Papademetris X, Shaywitz SE, Shaywitz BA, Constable RT. 2014 Disruption of functional networks in dyslexia: a whole-brain, data-driven analysis of connectivity. *Biol. Psychiat.* **76**, 397–404. (doi:10.1016/j.biopsych.2013.08.031)
25. Handa T, Mukuno K, Uozato H, Niida T, Shoji N, Shimizu K. 2004 Effects of dominant and nondominant eyes in binocular rivalry. *Optom. Vis. Sci.* **81**, 377–383. (doi:10.1097/01.opx.0000135085.54136.65)
26. Shneor E, Hochstein S. 2008 Eye dominance effects in conjunction search. *Vision Res.* **48**, 1592–1602. (doi:10.1016/j.visres.2008.04.021)
27. Pikovsky AS, Kurths J. 1997 Coherence resonance in a noise-driven excitable system. *Phys. Rev. Lett.* **78**, 775–778. (doi:10.1103/PhysRevLett.78.775)
28. Singh KP, Ropars G, Brunel M, Bretenaker F, Le Floch A. 2001 Stochastic resonances in an optical two-order parameter vectorial system. *Phys. Rev. Lett.* **87**, 213901. (doi:10.1103/PhysRevLett.87.213901)
29. Mori T, Kai S. 2002 Noise-induced entrainment and stochastic resonance in human brain waves. *Phys. Rev. Lett.* **88**, 218101. (doi:10.1103/PhysRevLett.88.218101)
30. Ando K., Kripke DF. 1996 Light attenuation by the human eyelid. *Biol. Psychiat.* **39**, 22–25. (doi:10.1016/0006-3223(95)00109-3)
31. Minucci PK, Connors MM. 1964 Reaction time under three viewing conditions: binocular, dominant eye, and nondominant eye. *J. Exp. Psychol. Gen.* **67**, 268–275. (doi:10.1037/h0039953)
32. Rombouts S, Barkhof F, Sprenger M, Valk J, Scheltens P. 1996 The functional basis of ocular dominance: functional MRI (fMRI) findings. *Neurosci. Lett.* **221**, 1–4. (doi:10.1016/S0304-3940(96)13260-2)
33. Corballis MC, Beale IL. 1976 *The psychology of left and right*. Hillsdale, NJ: Lawrence Erlbaum Associates.
34. Cornell JM. 1985 Spontaneous mirror-writing in children. *Can. J. Psychol.* **39**, 174–179. (doi:10.1037/h0080122)
35. McCloskey M, Rapp B. 2000 A visually based developmental reading deficit. *J. Mem. Lang.* **43**, 157–181. (doi:10.1006/jmla.2000.2724)
36. Dehaene S, Nakamura K, Jobert A, Kuroki C, Ogawa S, Cohen L. 2010 Why do children make mirror errors in reading? Neural correlates of mirror invariance in the visual word form area. *Neuroimage* **49**, 1837–1848. (doi:10.1016/j.neuroimage.2009.09.024)
37. Pegado F, Nakamura K, Cohen L, Dehaene S. 2011 Breaking the symmetry: mirror discrimination for single letters but not for pictures in the visual word form area. *Neuroimage* **55**, 742–749. (doi:10.1016/j.neuroimage.2010.11.043)
38. Borst G, Ahr E, Roell M, Houdé O. 2015 The cost of blocking the mirror generalization process in reading: evidence for the role of inhibitory control in discriminating letters with lateral mirror-image counterparts. *Psychon. Bull. Rev.* **22**, 228–234. (doi:10.3758/s13423-014-0663-9)
39. Zhang LI, Tao HW, Holt CE, Harris WA, Poo M. 1998 A critical window for cooperation and competition among developing retinotectal synapses. *Nature* **395**, 37–44. (doi:10.1038/25665)
40. Bishop DVM. 2015 The interface between genetics and psychology: lessons from developmental dyslexia. *Proc. R. Soc. B* **282**, 20143139. (doi:10.1098/rspb.2014.3139)
41. Carrion-Castillo A, Franke B, Fisher SE. 2013 Molecular genetics of dyslexia: an overview. *Dyslexia* **19**, 214–240. (doi:10.1002/dys.1464)
42. Hubel DH. 1988 *Eye, brain, and vision*. New York, NY: Scientific American Library.
43. Kremkow J, Jin J, Wang Y, Alonso JM. 2016 Principles underlying sensory map topography in primary visual cortex. *Nature* **533**, 52–57. (doi:10.1038/nature17936)
44. Dellatolas G, Curt F, Dargent-Paré C, De Agostini M. 1998 Eye dominance in children: a longitudinal study. *Behav. Genet.* **28**, 187–195. (doi:10.1023/A:1021471129962)
45. Jainta S, Kapoula Z. 2011 Dyslexic children are confronted with unstable binocular fixation while reading. *PLoS ONE* **6**, 18694. (doi:10.1371/journal.pone.0018694)
46. Field GD *et al.* 2010 Functional connectivity in the retina at the resolution of photoreceptors. *Nature* **467**, 673–677. (doi:10.1038/nature09424)
47. Cossell L, Iacaruso MF, Muir DR, Houlton R, Sader EN, Ko H, Hofer SB, Mrsic-Flogel TD. 2015 Functional organization of excitatory synaptic strength in primary visual cortex. *Nature* **518**, 399–403. (doi:10.1038/nature14182)
48. Lee KS, Huang X, Fitzpatrick D. 2016 Topology of ON and OFF inputs in visual cortex enables an invariant columnar architecture. *Nature* **533**, 90–94. (doi:10.1038/nature17941)
49. Pietrasanta M, Restani L, Caleo M. 2012 The corpus callosum and the visual cortex: plasticity is a game for two. *Neural Plast.* **2012**, 838672. (doi:10.1155/2012/838672)
50. Stein J. 2001 The magnocellular theory of developmental dyslexia. *Dyslexia* **7**, 12–36. (doi:10.1002/dys.186)
51. Mello NK. 1967 Inter-hemispheric comparison of visual stimuli in the pigeon. *Nature* **214**, 144–145. (doi:10.1038/214144a0)
52. Rollenhagen JE, Olson CR. 2000 Mirror-image confusion in single neurons of the macaque inferotemporal cortex. *Science* **287**, 1506–1508. (doi:10.1126/science.287.5457.1506)
53. Aasved H. 1987 Ophthalmological status of school children with dyslexia. *Eye* **1**, 61–68. (doi:10.1038/eye.1987.10)
54. Vidyasagar TR. 2013 Reading into neuronal oscillations in the visual system: implications for developmental dyslexia. *Front. Hum. Neurosci.* **7**, 811. (doi:10.3389/fnhum.2013.00811)
55. Paulesu E *et al.* 2001 Dyslexia: cultural diversity and biological unity. *Science* **291**, 2165–2167. (doi:10.1126/science.1057179)
56. McCrory EJ, Mechelli A, Frith U, Price CJ. 2005 More than words: a common neural basis for reading and naming deficits in developmental dyslexia. *Brain* **128**, 261–267. (doi:10.1093/brain/awh340)